# Realizing Magnetoelectric Coupling with Hydrogen Intercalation

J. Y. Ni, P. S. Wang, J. L. Lu, and H. J. Xiang*
*Key Laboratory of Computational Physical Sciences (Ministry of Education), State Key Laboratory of Surface Physics, and Department of Physics, Fudan University, Shanghai 200433, People's Republic of China and Collaborative Innovation Center of Advanced Microstructures, Nanjing 210093, People's Republic of China*

(Received 1 May 2018; revised manuscript received 25 December 2018; published 20 March 2019)

Materials with a coexistence of magnetic and ferroelectric order (i.e., multiferroics) provide an efficient route for the control of magnetism by electric fields. Unfortunately, a long-sought room temperature multiferroic with strongly coupled ferroelectric and ferromagnetic (or ferrimagnetic) orderings is still lacking. Here, we propose that hydrogen intercalation in antiferromagnetic transition-metal oxides is a promising way to realize multiferroics with strong magnetoelectric coupling. Taking brownmillerite $SrCoO_{2.5}$ as an example, we show that hydrogen intercalated $SrCoO_{2.5}$ displays strong ferrimagnetism and large electric polarization in which the hydroxide acts as a new knob to simultaneously control the magnetization and polarization at room temperature. We expect that ion intercalation will become a general way to design magnetoelectric and spintronic functional materials.

DOI: 10.1103/PhysRevLett.122.117601

Multiferroics [1–8] are attracting increasing interest not only due to the profound underlying physics (i.e., the coexistence and coupling of ferroelectric and magnetic orders) but also the potential applications in novel multifunctional devices. In particular, multiferroics may be used to realize nonvolatile, low-power, and high-density memory devices that combine fast electrical writing and magnetic reading. For such a purpose, an ideal multiferroic should have large ferroelectric polarization and large spontaneous magnetization at room temperature, and the magnetoelectric (ME) coupling should be strong [9].

Unfortunately, such high-performance multiferroics have not been realized experimentally. In the so-called type-II multiferroics [10–12] (e.g., $TbMnO_3$), the electric polarization caused by the noncentrosymmetric magnetic order is usually too small despite the intrinsic strong ME coupling. In type-I multiferroics in which the ferroelectricity and magnetism have different sources, the ME coupling is usually weak [9,13]. Interestingly, it was recently proposed [14,15] that the oxygen octahedral rotation can be utilized as a knob to control simultaneously the magnetism ($M$) and polarization ($P$). For instance, tuning the antiphase octahedral rotation in the hybrid improper ferroelectric material $Ca_3Mn_2O_7$ can not only affect the polarization arising from the trilinear coupling between polarization and two rotational modes, but it also changes the canted magnetic moment since the Dzyaloshinskii-Moriya interaction is correlated to the Mn-O-Mn angle. However, its magnetic critical temperature ($T_N = 118$ K) is low, and the canted magnetic moment is small, and the switch of its ferroelectric polarization has not been achieved experimentally. Hence, it will be interesting from both physics and application points of view to discover new mechanisms for realizing strong ME coupling.

In this Letter, we propose that "hydroxide" (i.e., the O-H covalent bond) can act as a knob to realizing ME coupling. To be more specific, the intercalation of the hydrogen ions can transform an antiferromagnetic (AFM) nonpolar material into a multiferroic with a large polarization and a high magnetization, and control the orientation of hydroxide results in a simultaneous change of magnetization and polarization. We demonstrate this general idea by considering the intercalation of hydrogen ions in brownmillerite $SrCoO_{2.5}$.

*General idea.*—Our general idea is illustrated in Fig. 1(a). One starts from a parent transition-metal oxide material which displays an AFM magnetic order with a high Néel temperature. Then we insert hydrogen ions into the parent material. The intercalated hydrogen ions will form O-H hydroxides. The hydroxide may deviate from the symmetric middle position, possibly in order to form an $O\cdots H$ hydrogen bond with the other neighboring $O^{2-}$ ion. As a result, there could be two possible configurations: hydroxide downward [left-hand panel of Fig. 1(a)] or hydroxide upward [right-hand panel of Fig. 1(a)]. Note that if all the transition-metal B ions in the parent material adopt the same valence state (i.e., $+n$), the $B^{n+}$ ion that is closest to the $H^+$ ion tends to become $B^{(n-1)+}$ to maintain the charge neutrality and minimize the Coulomb interaction. Since the $B^{(n-1)+}$ ion has a different magnetic moment from the $B^{n+}$ ion, these two configurations will have opposite total magnetic moments assuming that the parent material has a robust AFM order (i.e., the flop of the $H^+$ ion does not change the spin directions of all the $B^{n+}$ ions of the material). If these two configurations are insulating, their electric polarizations will also be different due to the different charge ordering

 

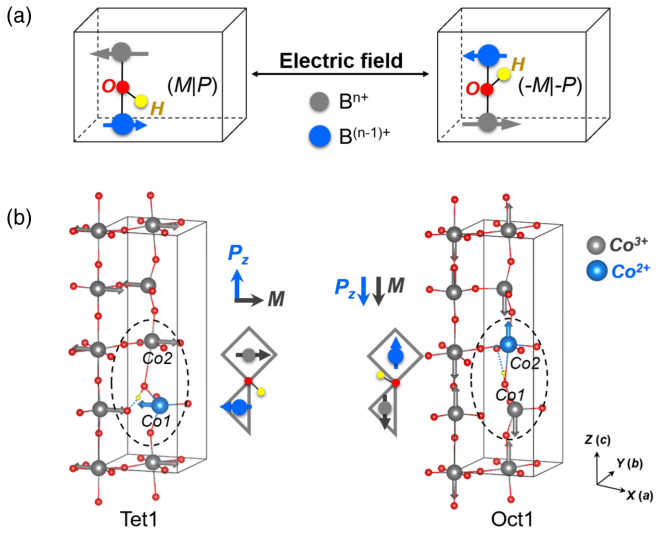


FIG. 1. (a) Illustration of the general idea of using hydroxide as a knob to simultaneously control the magnetization and polarization. Longer gray arrows and shorter blue arrows represent local magnetic moment of magnetic ions ($B^{n+}$ and $B^{(n-1)+}$), respectively. For clarity, only the two B ions near the hydroxide are shown. (b) ME coupling in $(SrCoO_{2.5})_8H_1$. Depending on the orientation of the hydroxide, two different configurations (left, tet1 configuration; right, oct1 configuration) have different net magnetization ($M$) and polarization ($P$). The local magnetic moments for each Co ion are displayed. The rhombus and triangle represent the oxygen octahedron and tetrahedron, respectively. Hydroxide and hydrogen bond are represented by solid and dotted line, respectively.

and different position of the $H^+$ ion. This suggests that an external electric field can switch between these two configurations. Therefore, hydroxide can serve as a knob to simultaneously manipulate the magnetization and polarization. There are three prerequisites to realize such an idea: (1) identify a parent transition-metal oxide with a robust AFM order, which is easy since most transition-metal oxides display a room temperature AFM order [16] (e.g., the $G$-type order); (2) one can intercalate hydrogen into the parent material; (3) the involved transition-metal ion of the parent transition-metal oxide should have the ability to change from one oxidation state to another; i.e., it presents multiple oxidation states.

*ME coupling in hydrogen-intercalated* $(SrCoO_{2.5})_8H_x$—. We will demonstrate the above idea with brownmillerite $SrCoO_{2.5}$ as the parent material. The brownmillerite structure can be derived from the $ABO_3$ perovskite oxides, by replacing 1/6 of oxygen ions by vacancies. The oxygen vacancies are ordered in such a way so that the tetrahedral $CoO_4$ layer and octahedral $CoO_6$ layer are alternatively stacked along the $c$ axis in $SrCoO_{2.5}$. $SrCoO_{2.5}$ displays a robust $G$-type AFM order below 537 K [17–19]. Recently, the ionic liquid gating technique was adopted to insert $H^+$ ions into $SrCoO_{2.5}$ to tune the optical and magnetic properties [19]. All these properties make $SrCoO_{2.5}$ an ideal parent material to realize the electric field control of magnetism with hydroxide as a knob. Note that $SrCoO_{2.5}$ might adopt different phases with varying tilting patterns of the $CoO_4$ tetrahedrons. Among the common two phases (*Pnma* and *Ima*2) [18], our density functional theory (DFT) calculations show that the *Pnma* phase has a lower energy by 54.88 meV/Co. Hereafter, we will mainly focus on the nonpolar *Pnma* phase of $SrCoO_{2.5}$. However, our test calculation shows that similar results on the hydroxide knob are obtained in the case of the *Ima*2 phase [see Sec. II of Supplemental Material (SM) [20]].

We will first consider the case when one hydrogen is added to the $SrCoO_{2.5}$ system, and then discuss the case of the presence of multiple hydrogens. For simplicity, we denote the structure of the $SrCoO_{2.5}$ unit cell (36 atoms in total) with one additional hydrogen as $(SrCoO_{2.5})_8H_1$. We will mainly report the results obtained with the Perdew-Burke-Ernzerhof functional since our tests show that the more accurate and demanding optB88_vdW functional [24] gives similar results (see Sec. III.1 of SM [20]). We determine the lowest-energy states [see Fig. 1(b)] of $(SrCoO_{2.5})_8H_1$ by considering all the possible absorption oxygen sites and orientations of hydroxide (Figs. S3 and S4 [20]). It turns out that the hydrogen ion will form a covalent O-H bond (i.e., hydroxide) with the bridge oxygen ion between the $CoO_4$ tetrahedron and the $CoO_6$ octahedron, in agreement with the previous result [19]. The formation energy calculations show that the hydrogen intercalation in $SrCoO_{2.5}$ is thermodynamically favorable [33], in agreement with the experimental observation [19]. We find that there are several locally stable states when the hydrogen ion is absorbed to the bridge oxygen since the hydroxide can rotate with respect to the oxygen to form a hydrogen bond with the other oxygen ions (Fig. S4 [20]). In the two lowest-energy states shown in Fig. 1(b), the hydroxide is orientated toward either the lower $CoO_4$ tetrahedron (referred to as tet1) or the upper $CoO_6$ octahedron (referred to as oct1), respectively. The tet1 state has a slightly lower energy than the oct1 state by 20 meV/H. For both states, the bond lengths of the O-H hydroxide and the O···H hydrogen bond are about 1 and 2 Å, respectively. Our first-principles molecule dynamics simulations indicate that tet1 and oct1 states are thermally stable at room temperature (Fig. S5 [20]). Our energy barrier calculations suggest that it is relatively easier to adjust the orientation of the hydroxide than to change the absorbed oxygen site of the hydrogen (Fig. S6 [20]). This is understandable since breaking the O···H hydrogen bond is much easier than breaking the covalent O-H bond.

In the parent material $SrCoO_{2.5}$, all the $Co^{3+}$ ions adopt the high-spin configuration (i.e., the local magnetic moment is close to 4 $\mu_B$). Our calculations show that the magnetic ground state of $SrCoO_{2.5}$ is the $G$-type magnetic ordering, in agreement with the experimental results [17–19]. For tet1 (oct1) configuration, the tetrahedral (octahedral) Co ion

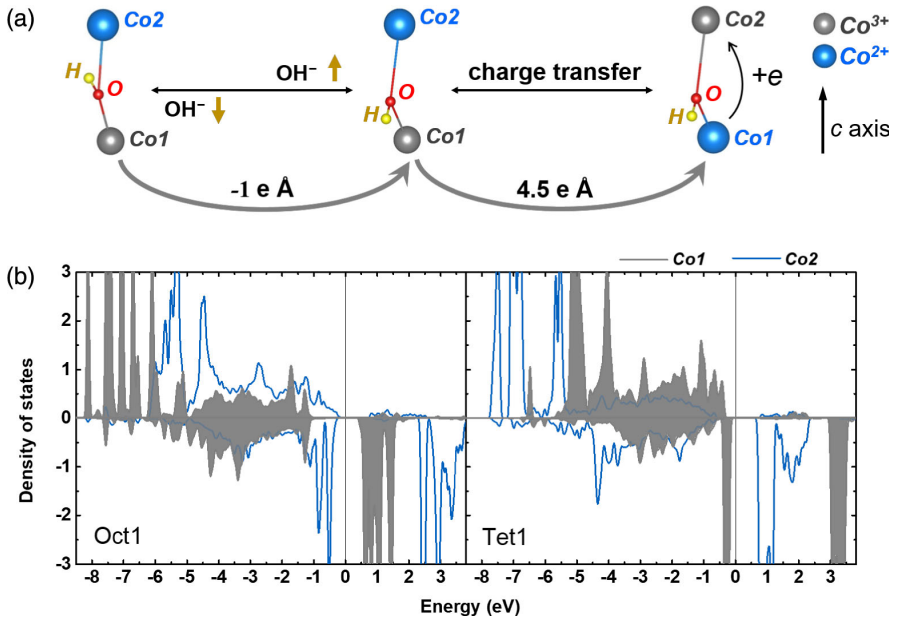


FIG. 2. Origin of the electric polarization difference between tet1 and oct1 configurations. (a) Simple estimation of the polarization change due to the hydroxide rotation and charge transfer associated with the charge ordering. Tetrahedral Co1 and octahedral Co2 are labeled in Fig. 1(b). (b) The partial DOS plot of the tetrahedral site Co1 (gray line) and the octahedral site Co2 (blue line) in the oct1 configuration (left) and tet1 configuration (right), evidencing the charge transfer associated with the charge ordering. In the DOS calculations, the *G*-type magnetic ordering is adopted. The positive and negative values represent majority component and spin minority component, respectively.

close to the hydroxide becomes the $Co^{2+}$ ion. We find that the $Co^{2+}$ ion also adopts a high-spin configuration with the local magnetic moment close to 3 $\mu_B$. The charge ordering pattern can also be seen from the density of state (DOS) analysis [see Fig. 2(b)]. We compute the spin exchange interactions (Tables S1 and S2 of SM [20]) with the four-state mapping method [27,28] to find that the $Co^{2+}$ spin couples antiferromagnetically with the neighboring $Co^{3+}$ spins. In fact, both tet1 and oct1 configurations adopt the *G*-type magnetic ordering [20]. Interestingly, the *G*-type magnetic ordering for both tet1 and oct1 configurations is ferrimagnetic instead of the usual AFM (e.g., $SrCoO_{2.5}$ [18]): Our DFT + *U* collinear spin-polarized calculation shows that the net magnetizations of the tet1 and oct1 configurations are 1 and $-1$ $\mu_B$ per unit cell, respectively. This is because the $Co^{2+}$ ion has a smaller local moment than the $Co^{3+}$ ion, and the neighboring Co spins are antiparallel to each other. By performing the Monte Carlo simulations, we estimate that the ferrimagnetic Curie temperatures of oct1 and tet1 configurations are all above 500 K (see Sec. III.3 of SM [20]).

We further consider the spin-orbit coupling effect to examine the magnetic anisotropy to find that the magnetic easy axes are along the *c* axis for purely $SrCoO_{2.5}$ and the oct1 configuration of $(SrCoO_{2.5})_8H_1$, while the magnetic easy axis of the tet1 configuration is along the *a* axis. To clearly understand how the orientation of the hydroxide affects the global magnetic anisotropy, we calculate single ion anisotropy (SIA) parameters of cobalt ions in $SrCoO_{2.5}$ and two configurations of $(SrCoO_{2.5})_8H_1$ (Tables S3–S5 [20]). For $SrCoO_{2.5}$, the SIA parameters show that the tetrahedral $Co^{3+}$ ions have strong magnetic easy-axis behavior along the *c* axis, while the spins of the octahedral $Co^{3+}$ ions prefer to be in the *ab* plane. Thus, there is a competition in the magnetic anisotropy between the two kinds of $Co^{3+}$. The reason why the magnetic easy axis is along the *c* axis for $SrCoO_{2.5}$ is that the tetrahedral $Co^{3+}$ ions have stronger magnetic anisotropy. For the magnetic anisotropy property in $(SrCoO_{2.5})_8H_1$, we find that the absorbed hydrogen ion mainly changes the SIA parameters of the two Co ions (Co1 and Co2 in Fig. S10 [20]) that bond with the oxygen ion of the hydroxide. For the oct1 configuration of $(SrCoO_{2.5})_8H_1$, the easy axis is still along the *c* axis despite the fact the magnetic easy-plane anisotropy of the octahedral Co2 ($Co^{2+}$) ion becomes stronger. However, in the tet1 configuration, the magnetic anisotropy of the $Co^{2+}$ ion (i.e., Co1 in Fig. S10 [20]) near the hydroxide changes: the easy axis is now along the *a* axis instead of the *c* axis. As a result, the magnetic easy axis of the tet1 configuration of $(SrCoO_{2.5})_8H_1$ is now along the *a* axis instead of the *c* axis. Therefore, the change of magnetic anisotropy of $(SrCoO_{2.5})_8H_1$ can be seen as a consequence of the local effect of the hydrogen intercalation. We note that both tet1 and oct1 configurations prefer to adopt collinear spin structures instead of noncollinear ones since the magnitudes of the antiferromagnetic exchange parameters (Tables S1–S5 [20]) are much larger than the SIA parameters.

Our calculations show that both tet1 and oct1 configurations have relatively large band gaps (0.95 and 0.74 eV, respectively). Since these two configurations differ in the orientation of the hydroxide and charge order pattern, there will be a nonzero electric polarization difference between the two configurations. With the Berry phase method [26], the difference in the out-of-plane electric polarization between tet1 and oct1 configurations is computed to be 18.79 $\mu C/cm^2$ along the [001] direction. This polarization value is close to that of proper ferroelectrics (e.g., $BaTiO_3$) [34], which is much larger than that of type-II multiferroics [10]. Note that the direction of the polarization is opposite to the orientation of the hydroxide: If we only consider the polarization contributed from the hydroxide, the difference in the out-of-plane electric polarization between tet1 and oct1 configurations should be along the $[00\bar{1}]$ direction since in the tet1 (oct1) case the hydroxide is orientated downward (upward). This is because the polarization difference is in fact mainly contributed by the charge ordering instead of the hydroxide position due to the large distance between the $Co^{2+}$ and $Co^{3+}$ ion along the $c$ axis. Our simple estimation [see Fig. 2(a)] shows that the electric polarization difference contributed from the rotation of the hydroxide is about $-1$ eÅ ($-3.41$ $\mu C/cm^2$), while the contribution from the charge ordering is 4.5 eÅ (15.35 $\mu C/cm^2$).

Our above results indicate that $(SrCoO_{2.5})_8H_1$ has two locally stable configurations with different magnetic properties and polarization associated with the different orientation of the hydroxide. We expect that an external electric field along the [001] direction can switch between the oct1 configuration and tet1 configuration due to the polarization difference. Because of the ME coupling mediated by the orientation of the hydroxide, the electric field can also switch the easy axis of the ferrimagnetic state. As these two configurations are not symmetrically equivalent, $(SrCoO_{2.5})_8H_1$ can be regarded as an asymmetric multiferroic [35] with a large magnetization and large electric polarization at room temperature. Note that here the ME coupling in $(SrCoO_{2.5})_8H_1$ with a fixed hydrogen amount is different from the phase transformation between AFM hydrogen-free $SrCoO_{2.5}$ and weakly ferromagnetic $(SrCoO_{2.5})_8H_8$ induced by the electric field [19].

Next, let us consider the case of inserting two hydrogens into $SrCoO_{2.5}$. In the case of the lowest-energy absorption pattern, there are four stable configurations which are named TT, TO, OT, and OO configurations, respectively (see Sec. IV of SM [20]). All these four configurations adopt $G$-type magnetic order as ground state. However, they adopt different charge ordering ground states: TO and OT configurations display the $G$-type charge ordering, while TT and OO configurations display the $C$-type charge ordering. Considering the charge order and spin order, the net magnetizations for TT, TO, OT, and OO configurations are 0, $-2$, 2, and 0 $\mu_B$ per unit cell, respectively. The magnetic easy axis is found to be along the $a$ axis for all four configurations. As shown in Fig. 3, four configurations of $(SrCoO_{2.5})_8H_2$ are very close in energy and four configurations have different magnetic and ferroelectric properties, suggesting that $(SrCoO_{2.5})_8H_2$ can be used as multiple-states memory, where the transformation between these states can be achieved with an electric field. Because of the entropy effect, the absorbed hydrogen ions may be disordered. To examine the effect of the disorder, we also consider the other two cases where the two hydroxides in $(SrCoO_{2.5})_8H_2$ are far from each other (see Sec. IV.4 of SM [20]). In these cases, we also find that hydroxide can act as a knob to simultaneously control the polarization and magnetization.

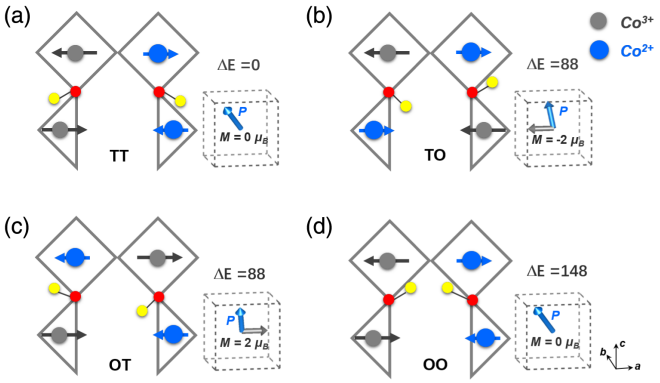


FIG. 3. Schematics of four configurations in $(SrCoO_{2.5})_8H_2$. (a) TT configuration: both hydroxides point toward oxygen tetrahedron, (b),(c) TO and OT configuration: one hydroxide points toward the octahedron, while the other points toward the tetrahedron, (d) OO configuration: both hydroxides point toward oxygen octahedron. All four configurations adopt the $G$-type magnetic structure with the easy axis along the $a$ axis as the magnetic ground state. Arrows denote the spin directions of the Co ions. Relative energies (meV/2H), net magnetization, and direction of total electric polarization are given for different configurations.

*Discussion.*—The multiferroic mechanism proposed in this work differs from the usual known mechanisms in several aspects. (1) The local electric dipole in hydrogen-intercalated AFM oxides is due to the orientation of the hydroxide and the associated charge order, resulting in a strong ME coupling. Although hydrogen-bond ordering was found to induce ferroelectricity in multiferroic systems such as $[(CH_3)_2NH_2]Mn(HCOO)_3$ [36], the magnetism hardly couples with the ferroelectricity. (2) Although charge order was suggested to induce ferroelectricity in some multiferroics [31,37,38], the ferroelectricity is hardly switchable by an external electric field since the conductivity in these systems appears to be too high due to a small band gap. In hydrogen-intercalated AFM oxides, the band gap could be rather large since the $H^+$ ion provides an additional attractive potential for the electron of the transition-metal ion close to the $H^+$ ion. For example, the band gap of $(SrCoO_{2.5})_8H_2$ is computed to be 1.2 eV. (3) A collective ordering of the hydroxide-related local electric dipoles in

hydrogen-intercalated AFM oxides is not necessary for realizing the coupling between the ferrimagnetism and electric dipole since an isolated hydroxide in an AFM oxide is itself stable at room temperature. This may suggest a new route to high-density storage with a single isolated hydroxide representing one bit. In contrast, the usual multiferroic displays a conventional ferroelectricity with a collective ordering of the local dipoles. (4) Besides $SrCoO_{2.5}$, we also find that hydroxide can act as a knob to simultaneously control the magnetization and polarization in other hydrogen-intercalated compounds (such as $CaFeO_{2.5}$ and perovskite $LaFeO_3$), indicating that the proposed ME coupling mechanism is general [39].

To summarize, we introduce a new knob—"hydroxide"—to simultaneously control magnetization and electric polarization in AFM transition-metal oxides. As we demonstrated in the cases of hydrogen-intercalated $SrCoO_{2.5}$, this idea leads to a new way to realize room temperature multiferroics in which the strong electric polarization and high magnetization are tightly coupled with each other. Our study suggests that ion intercalation is a promising way to rationally design new functional magnetoelectric and spintronic materials.

This work is supported by NSFC 11825403, the Special Funds for Major State Basic Research (Grant No. 2015CB921700), the Qing Nian Ba Jian Program, and the Fok Ying Tung Education Foundation. We thank Professor P. Yu and Mr. K. Liu for the useful discussion.

*hxiang@fudan.edu.cn

[1] S.-W. Cheong and M. Mostovoy, Nat. Mater. **6**, 13 (2007).
[2] W. Eerenstein, N. Mathur, and J. F. Scott, Nature (London) **442**, 759 (2006).
[3] R. Ramesh and N. A. Spaldin, Nat. Mater. **6**, 21 (2007).
[4] S. Picozzi and C. Ederer, J. Phys. Condens. Matter **21**, 303201 (2009).
[5] D. Rahmedov, D. Wang, J. Íñiguez, and L. Bellaiche, Phys. Rev. Lett. **109**, 037207 (2012).
[6] J. M. Rondinelli and C. J. Fennie, Adv. Mater. **24**, 1961 (2012).
[7] S. Dong, J.-M. Liu, S.-W. Cheong, and Z. Ren, Adv. Phys. **64**, 519 (2015).
[8] J. Varignon, N. C. Bristowe, and P. Ghosez, Phys. Rev. Lett. **116**, 057602 (2016).
[9] N. A. Spaldin, S.-W. Cheong, and R. Ramesh, Phys. Today **63**, No. 10, 38 (2010).
[10] T. Kimura, T. Goto, H. Shintani, K. Ishizaka, T.-h. Arima, and Y. Tokura, Nature (London) **426**, 55 (2003).
[11] A. Malashevich and D. Vanderbilt, Phys. Rev. Lett. **101**, 037210 (2008).
[12] H. J. Xiang, S.-H. Wei, M.-H. Whangbo, and J. L. F. Da Silva, Phys. Rev. Lett. **101**, 037209 (2008).
[13] J. Wang *et al.*, Science **299**, 1719 (2003).
[14] N. A. Benedek and C. J. Fennie, Phys. Rev. Lett. **106**, 107204 (2011).
[15] P. S. Wang, W. Ren, L. Bellaiche, and H. J. Xiang, Phys. Rev. Lett. **114**, 147204 (2015).
[16] D. Khomskii, *Transition Metal Compounds* (Cambridge University Press, Cambridge, England, 2014).
[17] T. Takeda, Y. Yamaguchi, and H. Watanabe, J. Phys. Soc. Jpn. **33**, 970 (1972).
[18] A. Muñoz, C. de La Calle, J. A. Alonso, P. M. Botta, V. Pardo, D. Baldomir, and J. Rivas, Phys. Rev. B **78**, 054404 (2008).
[19] N. Lu *et al.*, Nature (London) **546**, 124 (2017).
[20] See Supplemental Material at http://link.aps.org/supplemental/10.1103/PhysRevLett.122.117601 for computational details, ME coupling in $(SrCoO_{2.5})_8H_1$ based on the *Ima*2 $SrCoO_{2.5}$ parent phase, and additional results on $(SrCoO_{2.5})_8H_1$ and $(SrCoO_{2.5})_8H_2$, which includes Refs. [18,21–32].
[21] P. E. Blöchl, Phys. Rev. B **50**, 17953 (1994).
[22] G. Kresse and J. Furthmüller, Phys. Rev. B **54**, 11169 (1996).
[23] K. Hukushima and K. Nemoto, J. Phys. Soc. Jpn. **65**, 1604 (1996).
[24] T. Thonhauser, V. R. Cooper, S. Li, A. Puzder, P. Hyldgaard, and D. C. Langreth, Phys. Rev. B **76**, 125112 (2007).
[25] A. I. Liechtenstein, V. I. Anisimov, and J. Zaanen, Phys. Rev. B **52**, R5467 (1995).
[26] R. D. King-Smith and D. Vanderbilt, Phys. Rev. B **47**, 1651 (1993).
[27] H. J. Xiang, E. J. Kan, S.-H. Wei, M.-H. Whangbo, and X. G. Gong, Phys. Rev. B **84**, 224429 (2011).
[28] H. Xiang, C. Lee, H.-J. Koo, X. Gong, and M.-H. Whangbo, Dalton Trans. **42**, 823 (2013).
[29] P. S. Wang and H. J. Xiang, Phys. Rev. X **4**, 011035 (2014).
[30] J. Ireta, J. Neugebauer, and M. Scheffler, J. Phys. Chem. A **108**, 5692 (2004).
[31] H. J. Xiang and M. H. Whangbo, Phys. Rev. Lett. **98**, 246403 (2007).
[32] J. P. Perdew, K. Burke, and M. Ernzerhof, Phys. Rev. Lett. **77**, 3865 (1996).
[33] The formation energies of $(SrCoO_{2.5})_8$-$H_x$ are calculated using the follow expression: $E_f = E(SCOH_x)$-$E(SCO)$-$x/2\,E(H_2)$, where $E(SCOH_x)$, $E(SCO)$, and $E(H_2)$ are the total energy of $(SrCoO_{2.5})_8H_x$, parent $SrCoO_{2.5}$, and $H_2$ molecule, respectively. The calculated $E_f$ are $-1.1$ and $-1.8$ eV per unit cell for $x = 1$ and 2, respectively. The negative value of $E_f$ indicates that $(SrCoO_{2.5})_8H_x$ is synthesizable.
[34] J. Neaton and K. Rabe, Appl. Phys. Lett. **82**, 1586 (2003).
[35] X. Z. Lu and H. J. Xiang, Phys. Rev. B **90**, 104409 (2014).
[36] P. Jain, V. Ramachandran, R. J. Clark, H. D. Zhou, B. H. Toby, N. S. Dalal, H. W. Kroto, and A. K. Cheetham, J. Am. Chem. Soc. **131**, 13625 (2009).
[37] D. V. Efremov, J. Van Den Brink, and D. I. Khomskii, Nat. Mater. **3**, 853 (2004).
[38] J. Van Den Brink and D. I. Khomskii, J. Phys. Condens. Matter **20**, 434217 (2008).
[39] The details about the other hydrogen intercalated compounds, such as $LaFeO_3$-H, and $CaFeO_{2.5}$-H, will be published elsewhere.